Patch-based Cortical Source Modeling for EEG/MEG Distributed Source Imaging: A Simulation Study

Chang-Hwan Im

Department of Biomedical Engineering, Yonsei University, Wonju, Korea

Abstract

The present study introduces a new cortical patch-based source model for EEG/MEG cortical source imaging to consider anatomical constraints more precisely. Conventional source models for EEG/MEG cortical source imaging have used coarse cortical surface mesh or sampled small number of vertices from fine surface mesh, and thus they failed to utilize full anatomical information which nowadays we can get with sub-millimeter modeling accuracy. Conventional ones placed a single dipolar source on each cortical patch and estimated its intensity by means of various inverse algorithms; whereas the suggested cortical patch-based model integrates whole cortical area to construct lead field matrix and estimates current density that is assumed to be constant in each cortical patch. We applied the proposed and conventional models to realistic EEG data and compared the results quantitatively. The quantitative comparisons showed that the proposed model can provide more precise spatial descriptions of neuronal source distribution.

Key words : EEG, MEG, brain mapping, inverse problem, lead field construction, cortical source imaging

I. INTRODUCTION

Macrocolumns of tens of thousands of synchronously activated pyramidal cortical neurons are widely believed to be the main EEG and MEG generators because of the coherent distribution of their large dendritic trunks which are locally oriented in parallel, perpendicularly to the human cerebral cortical surface [1-3]. Nowadays, this physiological phenomenon has been successfully adopted and widely used as a basic anatomical constraint in EEG and MEG source imaging [4-11]. The source imaging with the anatomical constraint, which has been often called cortically distributed source model [12], resulted in elimination of spurious sources [13] as well as reduction of crosstalk distribution [14], compared to classical voxel (volume pixel) based imaging techniques.

To impose the anatomical constraint, many dipolar sources should be placed on cortical surface, usually on the interface between white and gray matter of the cerebral cortex extracted from structural MRI, which is relatively easier to be extracted than the other borders. We can further constrain each of these dipolar sources to be normal to the surface. Then, the strengths

Corresponding Author : Chang-Hwan Im, Ph.D.
Department of Biomedical Engineering, Yonsei University, 234
Maeji-ri, Heungup-myeon, Wonju-si, Kangwon-do, 220-710,
Korea
Tel : +82-33-760-2792 / Fax : +82-33-763-1953
E-mail : ich@yonsei.ac.kr

and/or orientations of the dipolar sources are determined using linear (L_2 norm) or nonlinear (L_p norm) estimation methods [4, 7]. To determine proper locations and orientations of the scattered sources, the cortical surface is usually tessellated into huge number of triangular elements, the number of which is often exceeding several hundreds of thousands. Developments of medical image processing techniques and high resolution structural MRI enabled us to get high resolution cortical surface with sub-millimeter modeling errors [15-17]. Unfortunately, however, it is computationally inefficient to use whole cortical surface vertices for the source reconstruction because of the increased underdetermined relationship between the limited numbers of measurements and the number of unknown variables to be reconstructed. To reduce the number of possible source locations, some people re-sampled the fine mesh to small number of larger triangles. Then, a unitary equivalent current dipole was placed in each node of the triangulated surface, with orientation parallel to the averaged normal vectors of the surrounding triangles [18, 19]. However, this kind of re-sampling approaches not only requires one more complex image processing procedure, but also has large possibility to lose accurate sulci-gyri structural information of the cortical surface. The other approach is to use a vertex-sampling process which has been frequently referred to as a *decimation* process [20-22]. Small number of vertices was down-sampled from the cortical surface as regularly as possible and used for source reconstruction purpose; whereas the original mesh information was used only

for visualization purpose. This approach is very simple to be applied, but it has some potential problems. First, the decimated vertices may not properly represent orientations of neighboring cortical vertices, especially around highly folded regions. This may result in significant reconstruction errors because neighboring dipolar sources with more appropriate orientations can be overestimated instead of the correct one due to crosstalk effect. Second, if the distribution of the decimated sources is irregular, the current intensity estimate can be distorted because density of the dipolar sources is inversely proportional to the estimated source intensity. Recently, Lin et al. [23] tackled this problem by incorporating patch areas in the forward model to yield estimates of the surface current density instead of dipole amplitudes at the current locations as well as adopting loose orientation constraint (LOC), which allows some variation of the current direction from the average normal. Their results showed that

the use of current density and LOC can improve overall accuracy of the source estimates.

In the present study, we have proposed an alternative source model to easily solve the problems of wrong orientation and irregular patch areas. Our approach does not use a single dipolar source that represents its neighboring vertices but uses all cortical vertices included in many small patches to construct lead field matrix. Since the constructed lead field matrix contains orientation and area information of all cortical vertices, the problems of the conventional approaches can be nicely solved.

II. METHODS

A. Conventional Source Model

As briefly described in the previous section, conventional source model has utilized reduced number of dipolar sources
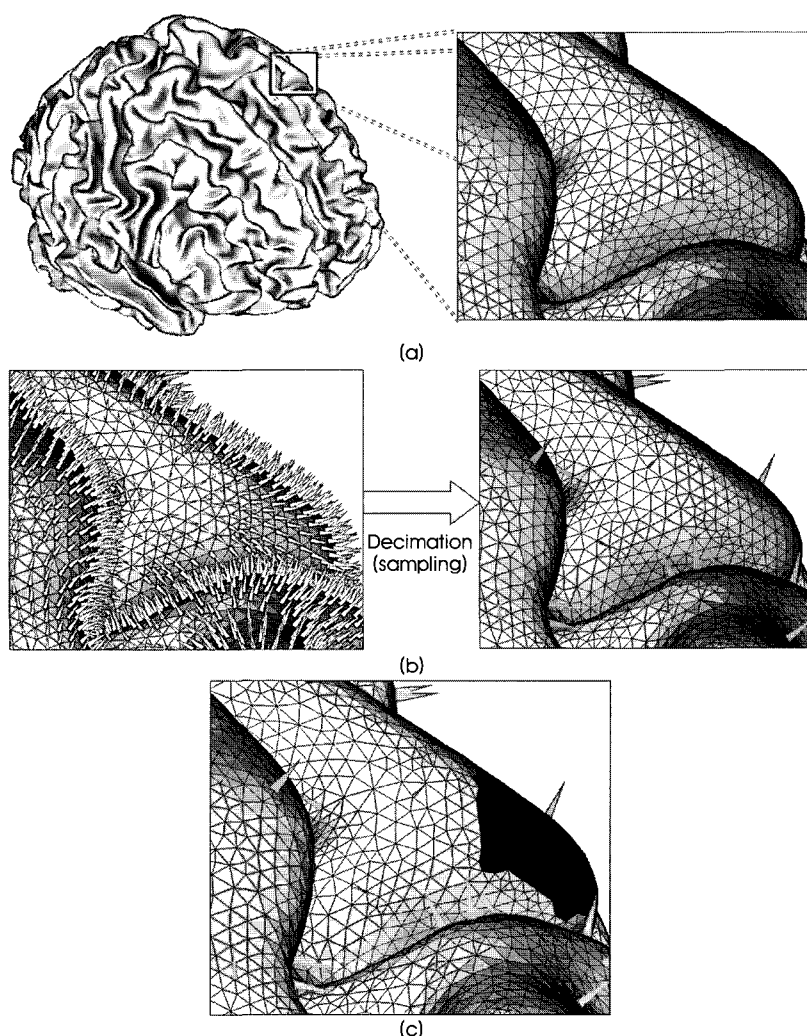

Fig. 1. An example of tessellated cortical surface and decimated sources: (a) cortical surface segmented and tessellated from an MRI T1 images (MNI standard brain); (b) original and decimated cortical vertices. 432,654 original vertices were reduced to 7,866 source positions; (c) area-of-influence around a decimated source (red vector). The orientation was determined by the vector sum of all vertices inside the patch.
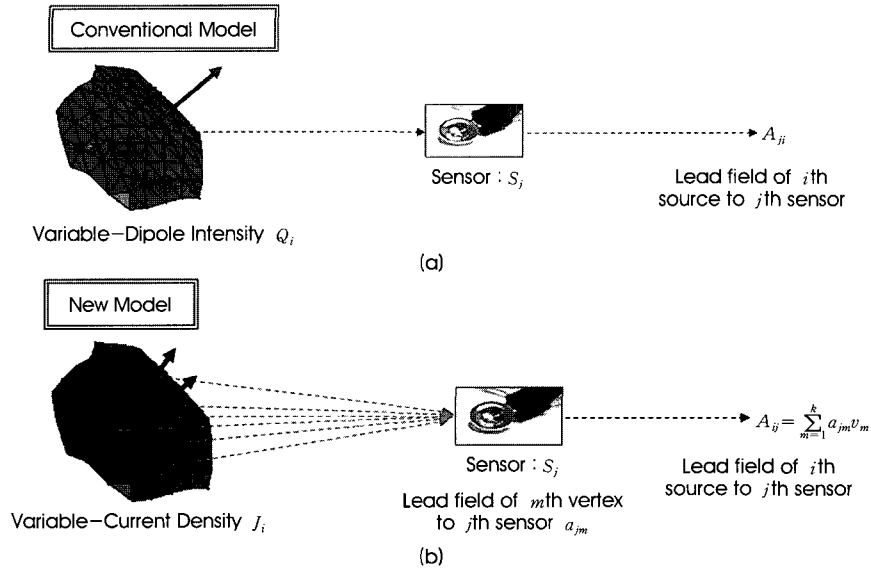
Fig. 2. Conceptual comparison between conventional and new source models: (a) conventional model uses a single dipolar source in a cortical patch to evaluate lead field matrix; (b) proposed model uses all vertices inside the cortical patch to evaluate the lead field matrix. Each vertex in the patch has its own unit normal vector $n_m = (n_{1m}, n_{2m}, n_{3m})$ and virtual area vm, where m = 1,···,k.

which were decimated from fine cortical surface structure. Figs. 1(a) and (b) show an example of the tessellated cortical surface and decimated source positions, in which 432,654 original vertices were reduced to 7,866 source positions. As seen in Fig. 1(c), a decimated vertex cannot properly represent orientations of its neighboring vertices, even when the dipole vector was determined by summing all neighboring vectors. We then evaluated the areas of patches and found that the size and shape of each patch are highly irregular[1] [23]. Thus, to use single dipolar sources to represent high resolution anatomical images may cause substantial errors in both forward calculation and inverse estimation of bioelectromagnetic sources.

The variable that has been used for the conventional source model is the moment intensity of each dipolar source when orientation constraint is imposed. Then, the relation between the dipole intensity and the measured data can be expressed according to the following system:

$$x = AQ + n \qquad (1)$$

where x is a column vector gathering the measurements on N_M sensors at a given time instant; Q is a column vector made of the N corresponding dipole intensities; A is the $N_M \times N$ lead field matrix; n is a perturbation or noise vector. The lead field A_{ji} is defined as electromagnetic quantity of jth sensor induced by ith dipolar source with unit intensity. Among various forward calculation methods, in this study, boundary element

1) The largest patch area is about 2 times larger than the smallest one.

method (BEM) considering realistic geometry head model was applied [24, 25].

B. Proposed Source Model

Contrary to the conventional source model, the proposed approach uses current density instead of the dipole intensity as a variable. First, the cortical surface is divided into N small cortical patches. Then, each cortical patch is assumed to have a constant current density J_i. In this case, the lead field A_{ji} is defined as electromagnetic quantity of jth sensor induced by ith cortical patch with unit current density. Suppose that the ith cortical patch includes k vertices. Each vertex has its own unit normal vector $n_m = (n_{1m}, n_{2m}, n_{3m})$ and virtual area v_m, where $m = 1, \cdots, k$. The virtual area was assigned to each vertex as a third of the area of all triangles meeting at a vertex [26]. This assumption is valid because the total virtual area remains equal to the actual area of the full tessellation. Then, we can evaluate the lead field a_{jm} defined as relationship between mth vertex and jth sensor by placing a unit dipole vector n_m at the position of the mth vertex. Eventually, the lead field at jth sensor by a unit current density in ith cortical patch is evaluated by integrating a_{mj} over the cortical patch as follows:

$$A_{ji} = \sum_{m=1}^{k} a_{jm} v_m \qquad (2)$$

Fig. 2 illustrates the conceptual comparison between the conventional and proposed source models. We can see from the figure that the new model can represent size, shape, and orien-

tation of each cortical patch without any loss of anatomical information.

Some previous studies have used similar concept of the constant cortical patch [6, 20], but they didn't aim for compensating anatomical information lost due to down-sampling of cortical vertices.

C. Forward Calculation and Inverse Estimation

In the present study, realistic geometry head model was considered to calculate electric potential induced by a point dipolar source [24, 25]. A three-layer boundary element model which consists of scalp, outer skull and inner skull was adopted [25, 27], which will be described again in the next section.

We used a linear estimation approach [4, 8] to reconstruct cortically distributed brain sources. The expression for the inverse operator W is

$$W = RA^T(ARA^T + \lambda^2 C)^{-1} \qquad (3)$$

where A is the lead field matrix, R is a source covariance matrix, and C is a noise covariance matrix. The source distribution can be estimated by multiplying the measured signal at a specific instant x by W. If we assume that both R and C are scalar multiples of identity matrix, this approach becomes identical to minimum norm estimation [28]. In this study, the source covariance matrix R was assumed to be a diagonal matrix, which means that we ignored relationships between neighboring sources. The lead field weightings [29] were imposed to each diagonal entry of R. In this study, pre-stimulus time window was used to calculate C. λ^2 is a regularization parameter and was determined systematically using the following equation [22]:

$$\lambda^2 = \frac{trace(ARA^T)}{trace(C)SNR^2} \qquad (4)$$

where $trace(.)$ and SNR represent sum of diagonal terms and signal to noise ratio, respectively. Although the equation (4) was derived from Bayesian inference theory [4, 28], the choice of the regularization parameter in (4) can be explained intuitively. The traces of matrices ARA^T and C were introduced to adjust the orders of the model term ARA^T and regularization term C in (3). The regularization parameter weakens the noise covariance term when SNR is high; while it strengthens the noise covariance term when SNR is low.

D. Computer Simulation

Neuroelectromagnetic inverse problems are hard to be verified by in-vivo experiments because exact source locations inside of the real human brain cannot be estimated a priori. For that reason, artificially constructed forward data are widely used to validate MEG and EEG inverse algorithms [6, 30]. Hence, we applied the proposed approach to artificially constructed EEG data.

We adopted realistic conditions to construct artificial EEG data. We assumed 128 electrodes that were attached on a subject's scalp according to extended 10-10 electrode system. To utilize anatomical information, interface between white and gray matter was extracted from MRI T1 images of an MNI standard brain (http://www.mrc-cbu.cam.ac.uk/Imaging/Common/mni space.shtml#evans_proc) and tessellated into 865,712 triangular elements and 432,654 vertices. To extract and tessellate the cortical surface, we applied BrainSuite developed in the University of Southern California, CA, USA [31]. For the accurate forward calculation, full head structures were taken into account and BEM was applied [28]. In the present study, the three-layer model, consisting inner and outer skull boundary and scalp surface, was used. 5,372 boundary elements and 2,748 surface nodes were generated from the same MRI data. The relative conductivity values of brain, skull, and scalp were assumed to be 1, 1/16, and 1, respectively [32]. Fig. 3 shows the boundary element model used in the present simulation.

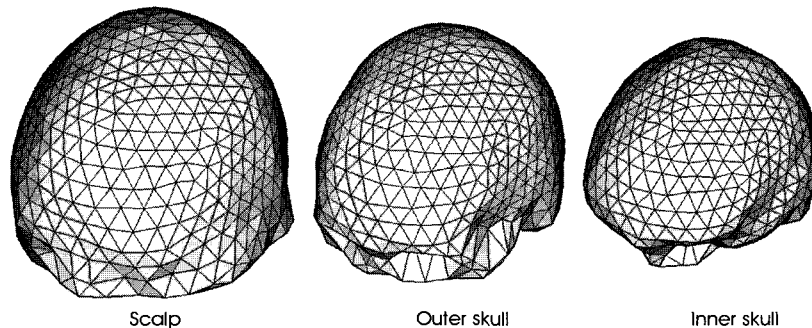Scalp   Outer skull   Inner skull

Fig. 3. Boundary element model for EEG forward calculations. 5,372 elements and 2,748 nodes were generated. Note that the cortical surface meshes were not included in the EEG forward calculation. They were used only for positioning dipolar sources.

Nowadays, for the forward simulations, generating artificial activation patches on a brain cortical surface has been popularized instead of activating some point sources [33]. To generate activation patches and construct forward data set, the concept of virtual area was adopted. The activation patch was generated using the following process: 1) A point is selected as a seed of an activation patch area. 2) The patch area is extended by including neighboring vertices around the patch. 3) If the total virtual area of the cortical patch exceeds an aimed surface area, the extension of the activation patch is terminated.

In the present study, we generated one activation patch for each simulation. The patch was made of a set of dipoles with constant current density and orientations perpendicular to the cortical surface. Then, the current dipole moment at each vertex was calculated by the product of the current density and the virtual area. The temporal variation of current density J was assumed as follows:

$$J = -0.6 \times 10^{-4}(t - 100)^2 + 0.6 \qquad (0\,ms \leq t < 200\,ms)$$
$$= 0 \qquad (200\,ms \leq t < 400\,ms)$$

After calculating electric potential at the 128-channel electrodes assuming 200 Hz-sampling rate, we added real brain noise, which was obtained from a pre-stimulus period of a practical EEG experiment. The original signal without noise was scaled in order for signal-to-noise ratio to be approximately 10 dB and 7 dB. Fig. 4 shows an example of the artificial EEG signals with respect to time.
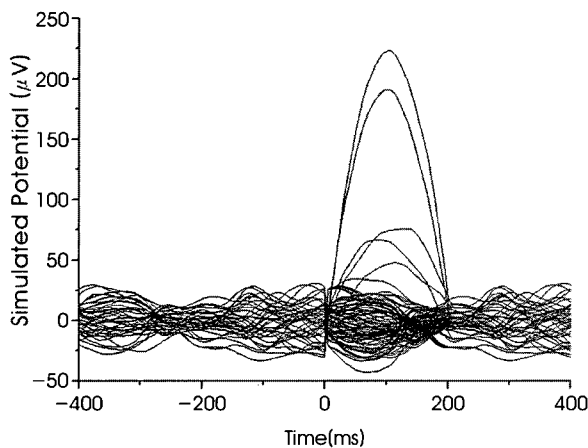

Fig. 4. An example of simulated EEG signals with real brain noise (SNR = 7 dB).

Although we used constant current patches to generate artificial EEG signals, they were not corresponding to the cortical patches used for the inverse estimation because they were generated independently using full tessellation of the cortical surface. In other words, the ideal patches of constant

activity do not recover exactly the patches considered in the source modeling.

E. Simulations and Results

We applied three different source models to the artificial EEG data. The three cases are as follows:

(Case 1) One dipolar source was placed on each patch, which is the conventional source model. The dipole intensity was used as a variable and the dipole orientation was determined by summing up normal vectors of neighboring vertices inside the patch.

(Case 2) One dipole source was placed on each patch as in the conventional source model, but area information of each patch was considered. Current density was used as a variable and area of each patch was multiplied by the conventional lead field. The dipole orientation was determined by summing up normal vectors of neighboring vertices inside the patch. This case was simulated to investigate the influence of different patch sizes on the solution accuracy.

(Case 3) Lead field matrix was evaluated by integrating all cortical vertices inside each patch, which is the present source model.

The three cases were tested for 50 activation patches of which the positions and sizes were randomly chosen. Two different SNRs, 10 dB and 7 dB, were simulated for each patch location. The same inverse method given in Eq. (3) was applied to the three cases. Fig. 5 and Fig. 6 show examples of results for two different patch locations when SNR was 7 dB. Each figure shows exact source location and source distributions reconstructed at 100 ms. Magnitude of the variables was normalized with respect to maximum value and sources that exceeded 0.1 were visualized. From the results, we can see the followings:

- When comparing the results of (Case 1) and (Case 2), we can see that the irregular distribution of patch sizes has just small influence on the solution accuracy. We can also see intuitively that emergence of small oscillatory sources was reduced slightly by using current density as a variable, which coincides well with a previous study [23].
- When the proposed source model was applied, the resultant distributions were more focalized compared to those of (Case 1) and (Case 2). Moreover, the shapes of the patches were more clearly reconstructed. Since the maximum magnitude was increased, many noisy sources had smaller normalized values than the cutoff magnitude (0.1) and removed from the visualization.

For more quantitative comparison, an assessment criterion named DF (degree of focalization) was introduced to measure
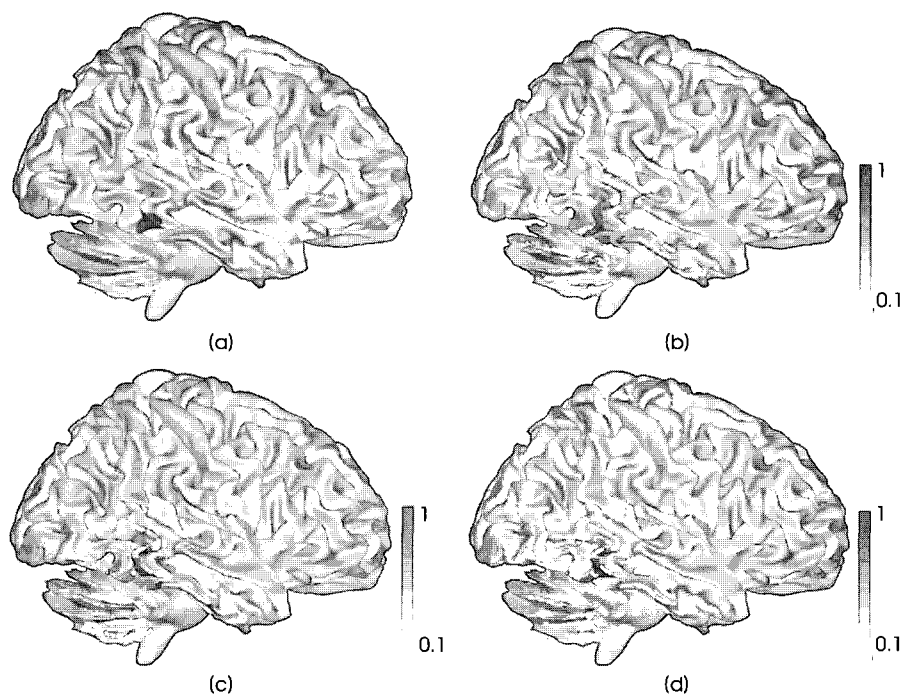
Fig. 5. Results of a realistic EEG simulation – a patch was assumed around right inferior temporal lobe: (a) Exact patch location; (b) Source distribution of (Case 1); (c) Source distribution of (Case 2); (d) Source distribution of (Case 3). All quantities were normalized with respect to their own maximum value. Sources that exceed 0.1 are visualized. SNR = 7 dB. DF values of (b), (c), and (d) are 0.081, 0.083, and 0.184, respectively.
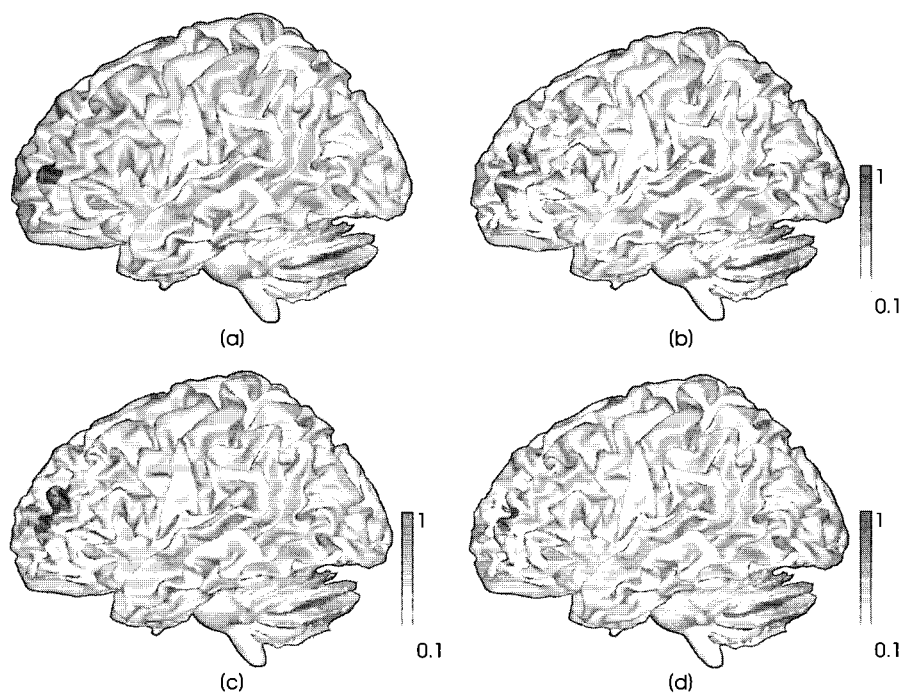

Fig. 6. Results of a realistic EEG simulation – a patch was assumed around left frontal lobe: (a) Exact patch location; (b) Source distribution of (Case 1); (c) Source distribution of (Case 2); (d) Source distribution of (Case 3). All quantities were normalized with respect to their own maximum value. Sources that exceed 0.1 are visualized. SNR = 7 dB. DF values of (b), (c), and (d) are 0.065, 0.069, and 0.153, respectively.

accuracy of the reconstructed source [33]. The DF is defined as energy reconstructed in a patch area divided by overall energy[2].

2) In this study, the integration was performed only for limited sources of which the magnitude exceeded 30% of maximum value because general minimum norm solution results in small DF values

If the energy in the assumed patch is exactly the same as that of whole source space, DF becomes 1. On the contrary, if the source is perfectly mislocalized, DF will be close to 0. Thus, higher DF implies that the method can reconstruct more accurate and focalized source distribution. This assessment criterion is similar to the ROC curve analysis which investigates relationship between true positive fraction and false positive fraction [18]. Fig. 7 shows the comparison of the DF values averaged for 50 activation patch simulations with different patch sizes and locations. The DF values decreased as the SNR increased, but the overall tendencies remained unchanged. We applied t-test to verify statistical difference of DF values between new and conventional source models. The t-test applied from (Case 1) and (Case 2) against (Case 3) stated statistical differences (p < 0.0005), while the (Case 1) and (Case 2) does not differ in their mean DF values (p > 0.1). It can be seen from the results that the proposed source model could result in more focalized and accurate source distribution very consistently. These results demonstrate that the orientation errors affect solution accuracy much more than irregular patch size does.
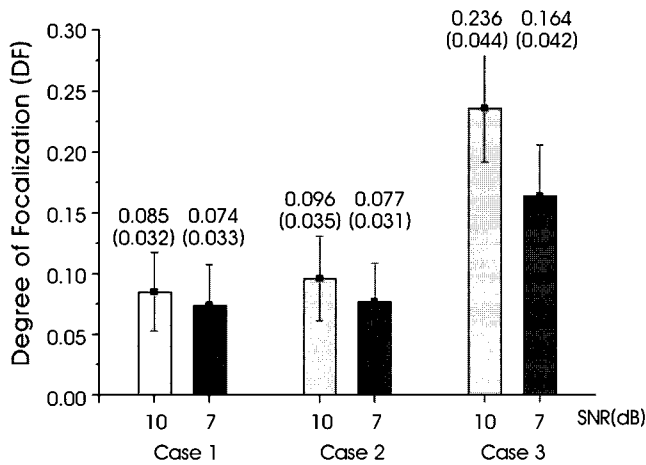

Fig. 7. Comparison of DF values averaged for 50 cortical patch simulations. Values in parentheses are standard deviations.

III. DISCUSSION

M any researchers have been trying to make the spatial resolution of EEG and MEG comparable to that of fMRI or PET, which is believed to have higher spatial resolution than EEG or MEG. As for hardware aspect, more and more researchers are moving to a higher number of channels, and EEG acquisition systems with 128 channels are not uncommon any more. Even 256 channel EEG systems are commercially available now [34]. In case of MEG, over 250 channel systems have been already popularized (e.g. CTF 275 MEG system) and being widely used. Combination of different modalities is now becoming a new alternative to enhance the limited spatial resolution of the electromagnetic-based imaging techniques [8]. As for software aspect, a lot of source imaging algorithms have been developed to get more accurate and focalized source estimate. Many methods are now adopting brain anatomy as a basic constraint because high resolution structural MRI technology and image processing techniques enable us to get more accurate information on the human brain anatomy [15, 17].

The present study deals with a problem arising when imposing the anatomical constraint. Conventional studies have generated coarse cortical surface mesh or sampled some vertices from fine cortical surface mesh, to place the dipolar sources, but either model could not take full advantage of the accurate anatomical information which currently has sub-millimeter accuracy. The conventional model placed one dipolar source in each cortical patch and estimated the dipole intensity; whereas the proposed model utilizes every cortical vertex inside a cortical patch in evaluating a lead field matrix and estimates the current density of the patch. Since the proposed model can be regarded as a kind of numerical integrations over each source patch, it can consider more accurate shapes and orientations of the cortical patches.

It seems obvious from (2) that the proposed model needs more computation to evaluate the lead field matrix than the conventional decimated source model. Nevertheless, the overall increment of computational time is not significant because the size of the lead field matrix constructed using the proposed model is the same as that of the conventional one. Please note that the most time-consuming processes are matrix multiplications and inversion in (3) and calculation of inverse stiffness matrix of boundary elements, which are common processes in both approaches. In the present simulations shown in Fig. 5, evaluation of (Case 1) took 54.3 s and that of (Case 3) took 55.5 s under a Pentium 4~3.4 GHz, Fortran 90 environment, where we can see that the difference is nearly negligible.

In the present study, the proposed model has been applied to realistic EEG simulations and the results have been compared to those of conventional ones. Boundary element method considering realistic geometry head model was used for the forward calculations. For the verification, we generated 50 cortical patches with different sizes and locations, and simulated time-varying EEG signals. To be more realistic, real brain noise extracted from a pre-stimulus period of a practical experiment was added to the artificial EEG signals. For the quantitative comparisons, we adopted a criterion named DF, which can measure how well the reconstructed sources recover the original patches. We could see from the simulations that the consideration of area information did not improve the results as much as we expected. However, the application of the proposed model

resulted in more accurate source estimate.

The proposed model is more plausible than the conventional ones because it considers whole cortical surface area without any loss of anatomical information. The present study only applied a linear inverse operator to the inverse estimation, but the proposed model is applicable to other inverse techniques that use same anatomical constraint because this model does not deal with forward or inverse calculation methods but just construction of lead field matrix containing more accurate anatomical information. Although the simulations were performed only for EEG, the model can be applied to MEG source estimation in the same manner.

In summary, we have used a source patch model that can consider accurate anatomical information in EEG/MEG cortical source imaging process. The proposed model has been applied to realistic EEG simulations and compared quantitatively with conventional ones. The present simulation results show that the proposed model provides enhanced performance in reconstructing cortical activations, as compared with conventional cortical source models. It is expected that the present model will serve as a useful means to get high resolution cortical source images in various EEG/MEG applications.

REFERENCES

[1]   P. L. Nunez and R. B. Silberstein, "On the relationship of synaptic activity to macroscopic measurements: Does co-registration of EEG with fMRI make sense?", Brain Topogra., Vol.13, pp.79-96, 2000.

[2]   B. He, Modeling and Imaging of Bioelectric Activity: Principles and Applications, Kluwer Academic/Plenum Publishers, 2004.

[3]   B. He, Neural Engineering, Kluwer Academic/Plenum Publishers, 2005.

[4]   A.M. Dale and M.I. Sereno, "Improved localization of cortical activity by combining EEG and MEG with MRI surface reconstruction: a linear approach", J. Cogn. Neurosci., Vol. 5, pp.162-176, 1993.

[5]   H. Buchner, G. Knoll, M. Fuchs, A. Rienäcker, R. Beckmann, M. Wagner, J. Silny, and P. Jorg, "Inverse localization of electric dipole current sources in finite element models of the human head", Electroenceph. Clin. Neurophysiol., Vol. 102, pp.267-278, 1997.

[6]   W.E. Kincses, C. Braun, S. Kaiser, and T. Elbert, "Modeling extended sources of event-related potentials using anatomical and physiological constraints", Hum. Brain Mapp., Vol. 8, pp. 182-193, 1999.

[7]   M. Fuchs, M. Wagner, T. Kohler, and H.A. Wischmann, "Linear and nonlinear current density reconstructions", J. Clin. Neurophysiol., Vol. 16, pp.267-295, 1997.

[8]   A.M. Dale, A.K. Liu, B.R. Fischl, R.L. Buckner, J.W. Belliveau, J.D. Lewine, and E. Halgren, "Dynamic Statistical Parametric Mapping: Combining fMRI and MEG for High-Resolution Imaging of Cortical Activity", Neuron, Vol. 26, pp.55-67, 2000.

[9]   C. Babiloni, "Linear inverse source estimate of combined EEG and MEG data related to voluntary movements", Hum. Brain Mapp., Vol. 14, pp.197-209, 2001.

[10] F. Babiloni, C. Babiloni, F. Carducci, G.L. Romani, P.M. Rossini, L.M. Angelone, and F. Cincotti, "Multimodal integration of high-resolution EEG and functional magnetic resonance imaging data: a simulation study", Neuroimage, Vol. 19, pp.1-15, 2003.

[11] S. Baillet, J.J. Riera, G. Marin, J.F. Mangin, J. Aubert, and L. Garnero, "Evaluation of inverse methods and head models for EEG source localization using a human skull phantom", Phys. Med. Biol., Vol. 46, pp.77-96, 2001.

[12] S. Baillet, J.C. Mosher, and R.M. Leahy, "Electromagnetic Brain Mapping", IEEE Signal Process. Mag., No. 11, pp.14-30, 2001.

[13] S. Baillet, Toward Functional Brain Imaging of Cortical Electrophysiology Markovian Models for Magneto and Electroencephalogram Source Estimation and Experimental Assessments, University of Paris XI : Ph. D. dissertation, 1998.

[14] A.K. Liu, J.W. Belliveau, and A.M. Dale, "Spatiotemporal imaging of human brain activity using functional MRI constrained magnetoencephalography data: Monte Carlo simulations", Proc. Natl. Acad. Sci. USA, Vol. 95, pp.8945-8950, 1998.

[15] A.M. Dale, B. Fischl, and M.I. Sereno, "Cortical Surface-Based Analysis I. Segmentation and Surface Reconstruction", Neuroimage, Vol. 9, pp.179-194, 1999.

[16] B. Fischl, M.I. Sereno, and A.M. Dale, "Cortical Surface-Based Analysis II. Inflation, Flattening, and a Surface-Based Coordinate System", Neuroimage, Vol. 9, pp.195-207, 1999.

[17] B. Fischl and A.M. Dale, "Measuring the thickness of the human cerebral cortex from magnetic resonance images", Proc. Natl. Acad. Sci. USA, Vol. 97, pp.11050-11055, 2000.

[18] F. Darvas, D. Pantazis, E. Kucukaltun-Yildirim, and R.M. Leahy, "Mapping human brain function with MEG and EEG: methods and validation", Neuroimage, Vol. 23, pp.S289-S299, 2004.

[19] F. Babiloni, F. Cinocotti, C. Babiloni, F. Carducci, D. Mattia, L. Astolfi, A. Basilisco, P.M. Rossini, L. Ding, Y. Ni, J. Cheng, K. Christine, J. Sweeney, and B. He, "Estimation of the cortical functional connectivity with the multimodal integration of high-resolution EEG and fMRI data by directed transfer function", Neuroimage, Vol. 24, pp.118-131, 2005.

[20] O. David and L. Garnero, "Time-Coherent Expansion of MEG/ EEG Cortical Sources", Neuroimage, Vol. 17, pp.1277-1289, 2002.

[21] R.P. Dhond, K. Marinkovic, A.M. Dale, T. Witzel, and E. Halgren, "Spatiotemporal maps of past-tense verb inflection", Neuroimage, Vol. 19, pp.91-100, 2003.

[22] F.H. Lin, T. Witzel, M.S. Hämäläinen, A.M. Dale, J.W. Belliveau, and S.M. Stufflebeam, "Spectral spatiotemporal imaging of cortical oscillations and interations in the human brain", Neuroimage, Vol. 23, pp.582-595, 2004.

[23] F.H. Lin, J.W. Belliveau, A.M. Dale, and M.S. Hämäläinen, "Distributed current estimates using cortical orientation constraints", Hum. Brain Mapp., Vol. 27, pp.1-13, 2006.

[24] B. He, T. Musha, Y. Okamoto, S. Homma, Y. Nakajima, and T. Sato, "Electric dipole tracing in the brain by means of the boun-

dary element method and its accuracy", IEEE Trans. Biomed. Eng., Vol. 34, pp.406-414, 1987.

[25] M.S. Hämäläinen and J. Sarvas, "*Realistic conductivity geometry model of the human head for interpretation of neuromagnetic data*", IEEE Trans. Biomed. Eng., Vol. 36, pp.165-171, 1989.

[26] M. Chupin, S. Baillet, C. Okada, D. Hasboun, and L. Garnero, "*On the detection of hippocampus activity with MEG.*", Proc. Int. Conf. Biomagnetism (BIOMAG2002), 2002.

[27] B. He, X. Zhang, J. Lian, H. Sasaki, D. Wu, and V.L. Towle, "*Boundary element method-based cortical potential imaging of somatosensory evoked potentials using subjects' magnetic resonance images*", Neuroimage, Vol. 16, pp.564-576, 2002.

[28] A.K. Liu, A.M. Dale, and J.W. Belliveau, "*Monte Carlo simulation studies of EEG and MEG localization accuracy*", Hum. Brain Mapp., Vol. 16, pp.47-62, 2002.

[29] I.F. Gorodnistky, J.S. George, and B.D. Rao, "*Neuromagnetic imaging with FOCUSS: a recursive weighted minimum norm algorithm*", Electroencephal. Clin. Neurophysiol., Vol. 95, pp.231-251, 1995.

[30] K. Sekihara, S.S. Nagarajan, D. Poeppel, A. Marantz, Y. Miyashita, "*Reconstructing spatio-temporal activities of neural sources using an MEG vector beamformer technique*", IEEE Trans. Biomed. Eng., Vol. 48, pp.760-771, 2001.

[31] D.W. Shattuck and R.M. Leahy, "*BrainSuite: An automated cortical surface identification tool*", Med. Image Anal., Vol. 6, pp.129-142, 2002.

[32] J. Haueisen, C. Ramon, M. Eiselt, H. Brauer, and H. Nowak, "*Influence of tissue resistivities on neuromagnetic fields and electric potentials studied with a finite element model of the head*", IEEE Trans. Biomed. Eng., Vol. 44, pp.727-735, 1997.

[33] C.H. Im, K.O. An, H.K. Jung, H. Kwon, Y.H. Lee, "*Assessment criteria for MEG/EEG cortical patch tests*", Phys. Med. Biol., Vol. 48, pp.2561-2573, 2003.

[34] E. Suarez, M.D. Viegas, M. Adjouadi, and A. Barreto, "*Relating induced changes in EEG signals to orientation of visual stimuli using the ESI-256 machine*", Biomed. Sci. Instrum., Vol. 36, pp. 33-38, 2000.